Appl Phys B
DOI 10.1007/s00340-010-3975-0

Applied Physics B
Lasers and Optics

QEPAS detector for rapid spectral measurements

A.A. Kosterev · P.R. Buerki · L. Dong · M. Reed · T. Day · F.K. Tittel

Received: 10 February 2010

Abstract A quartz enhanced photoacoustic spectroscopy sensor designed for fast response was used in combination with a pulsed external cavity quantum cascade laser to rapidly acquire gas absorption data over the 1196–1281 cm^{-1} spectral range. The system was used to measure concentrations of water vapor, pentafluoroethane (freon-125), acetone, and ethanol both individually and in combined mixtures. The precision achieved for freon-125 concentration in a single 1.1 s long spectral scan is 13 ppbv.

1 Introduction

Quartz enhanced photoacoustic spectroscopy (QEPAS) [1, 2] is based on the use of a quartz tuning fork (QTF) as a detector for acoustic oscillations induced in an absorbing gas by modulated optical radiation. Readily available QTFs designed for timing applications and oscillating at ∼32.8 kHz (i.e., close to 2^{15} Hz) were used in all the QEPAS work reported to date. A QTF is an oscillator with extremely low internal losses; its quality factor Q in vacuum is typically 70 000 to 110 000. In QEPAS applications, the QTF is immersed in gas, which dampens its motion. Nevertheless, the typical Q of a QTF in air at normal pressure and temperature conditions is still very high, i.e., ∼10 000 to 13 000. While the high Q of a QTF detector is helpful for obtaining an enhanced signal to noise ratio (SNR), it limits the response time of the detector. As is well known from classical oscillator theory,

$$\tau = \frac{Q}{\pi f_0} \tag{1}$$

where f_0 is the natural vibration frequency of the oscillator and τ is the time needed for the vibration amplitude to decay to $1/e$ of the initial value. Consequently, the response time of a QTF in ambient air is $\tau \sim 100$ ms, and uncorrelated measurements can be taken in ∼300 ms intervals. This time is too long for a rapid scans technique often used in absorption spectroscopy with photodiodes or other fast detectors. This does not prevent QEPAS from achieving a high sensitivity when applied to the detection of small molecules. QEPAS features zero baseline, practically no $1/f$ noise, and its sensitivity is not limited by the laser source noise. With a properly designed optical system and a spatially clean optical excitation source, a QEPAS detector was shown to perform at the QTF thermal noise limit. However, there are situations where a faster response time is desired. One such case is when it is not possible to achieve a zero baseline level. The spatial distribution of radiation from many kinds of laser sources has wide spread low intensity wings even if most of the emitted power is concentrated in the near-Gaussian central beam. Radiation from these wings results in a non-zero background when absorbed in the spectrophone structural elements. A noticeable signal background is usually present when amplitude modulation (AM) instead of wavelength modulation (WM) is used.

The most often used QEPAS spectrophone design is shown in Fig. 1, consisting of a QTF and two symmetrically positioned pieces of thin rigid tubing which form an

A.A. Kosterev (✉) · L. Dong · F.K. Tittel
Department of Electrical and Computer Engineering, Rice University, MS-366, 6100 Main Street, Houston, TX 77251, USA
e-mail: akoster@rice.edu

P.R. Buerki · M. Reed · T. Day
Daylight Solutions, Inc., 13029 Danielson Street, Suite 130, Poway, CA 92064, USA

Published online: 16 March 2010

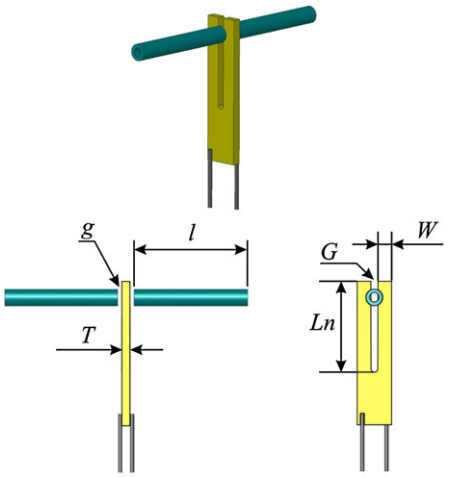

Fig. 1 Spectrophone design and definitions of the dimensions. G is width of the opening between the QTF prongs, and g is the gap between a microresonator tube facet and the QTF

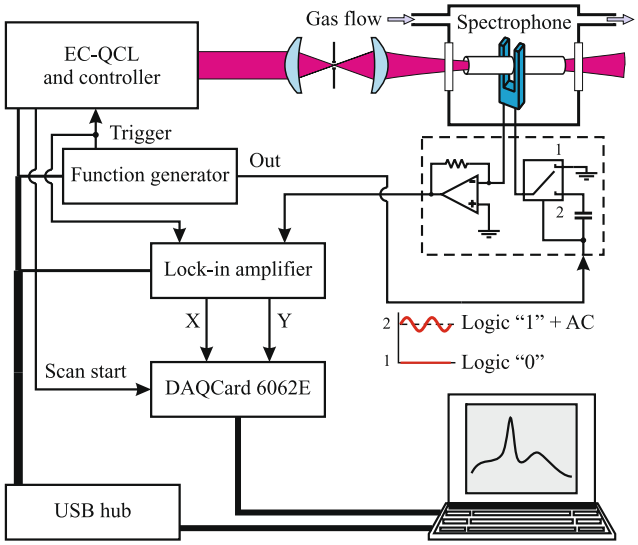

Fig. 2 Sensor schematic. *Dashed box* represents the transimpedance amplifier and an electronic switch circuit board. High logic level sets the switch in position 2, where an external AC voltage can be applied to the QTF. Function generator: DS345, lock-in amplifier: SR844, both from Stanford Research Systems

acoustic microresonator. In a QEPAS review paper [2] published in 2005, it was assumed that the microresonator does not significantly affect the QTF properties (i.e. f_0 and Q). That statement was experimentally verified and valid for the μRs used at that time, with the length of each tube $l \approx \lambda_s/4$, where λ_s is the sound wavelength, and for pressures of ∼100 Torr or less, which the authors then believed to represent the optimal conditions. Our recent research, however, revealed that acoustic resonance in a microresonator of this geometry occurs when $l \approx \lambda_s/2$. In this case and at higher pressures (∼1 atm), the microresonator strongly impacts the QTF parameters, reducing the quality factor to 1500–2500 and at the same time improving the fundamental absorption detection limit [3]. Then according to (1), $\tau \sim 20$ ms, and relatively fast spectral measurements are possible. In this paper, we shall describe a QEPAS sensor using a rapidly tunable external cavity quantum cascade laser (EC-QCL) as an excitation source to detect and quantify molecules with wide and quasi-unstructured absorption bands. The spectral signatures of atmospheric water vapor will also be measured at different spectral scan rates.

2 Experimental setup

A schematic of the QEPAS gas sensor using an EC-QCL (Daylight Solutions, Inc., Tunable Pulsed External Cavity Quantum Cascade Laser—ECqcL™, model No. 11080) as an excitation source is shown in Fig. 2. The laser operated in a pulsed mode. The repetition rate was adjusted to match the resonant frequency, $f_0 \approx 32\,760$ Hz of the QTF located in the spectrophone. The maximum technically possible laser pulse width at this frequency was 2.14 ms (7% duty cycle). According to the manufacturer's specifications and our tests described in the next section, the EC-QCL was continuously tunable in the 1196–1281 cm^{-1} spectral range. The slowest spectral scan allowed by the laser driver takes 6.5 s in one direction, and the scan rate could be changed in integer multiples up to ×6. Thus, the fastest scan covered the full 85 cm^{-1} tuning range in ∼1.1 s at a scan rate of 77.3 cm^{-1}/s, while the ×1 scan rate was 12.9 cm^{-1}/s. The laser radiation was spatially filtered and focused into the spectrophone center using two germanium meniscus lenses, each with a 16.5 mm focal length. Either a 150 μm or a 200 μm diameter pinhole was installed at the focal point between the two lenses. During the measurements the EC-QCL was scanned bi-directionally over its full tuning range, but only one direction was used for collecting the spectral data.

The QTF signal was detected using a transimpedance amplifier with a 10 MΩ feedback resistor as reported in previous QEPAS publications (see, for example, [2] and references therein). The amplifier board (25 × 45 mm^2) was positioned close to the spectrophone and contained as well an electronic switch which allowed excitation of the QTF by an external electrical signal. This feature was used to measure the main QTF electrical parameters: its stray electrical capacitance $C_\parallel$, f_0, Q, and its dynamic resistance R. The measurements were performed as follows. First, electrical excitation at a 25 kHz frequency far from the QTF resonance was applied. At this frequency, the current through the QTF I is $I = U \times i\omega C_\parallel$, thus allowing the determination of $C_\parallel$. Then the frequency region near the QTF resonance was scanned, and the calculated capacitive $C_\parallel$ current

Table 1 Parameters of the two spectrophones (SPh#1 and SPh#2) used in this work. All dimensions are in mm. *ID*, *OD*—inner and outer diameters of the microresonator tubes. The QTFs are identical to the one used in [4] with $Ln = 3.8$ mm, $T = 0.34$ mm, $W = 0.6$ mm, and $G = 0.3$ mm (see Fig. 1). All the microresonator tubes are mounted with $g \approx 0.03$ mm, and the measurements were performed at 750 Torr pressure. The relative humidity of the sampled ambient air was 43% at +20°C (1% H_2O vapor concentration by volume). The τ is the spectrophone response time at $1/e$ amplitude decay level, calculated based on f_0 and Q

SPh	*ID*	*OD*	*l*	f_0, Hz	Q	τ, ms	R, kΩ	C, fF	L, kH
#1, dry N_2	0.51	0.81	4.3	32739.20	3125	30	409.2	3.80	6.22
#1, air				32738.51	4293	42	299.4	3.78	6.25
#2, dry N_2	0.84	1.27	4.0	32759.54	1380	13	863.1	4.07	5.79
#2, air				32761.04	1958	19	625.7	3.97	5.95

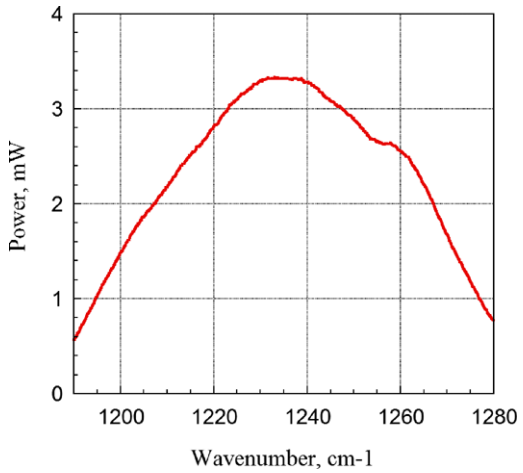

Fig. 3 The laser power measured behind the spectrophone cell as a function of the wavenumber at the slowest scan speed (×1, 12.9 cm^{-1}/s)

subtracted from the measured current. The resulting resonance curve $I^2(f)$ was fitted with a Lorentzian function and used to determine f_0, $Q = \frac{f_0}{\Delta f}$ and $R = \frac{U}{I_{max}}$. Based on these numbers, other relevant electrical parameters of the QTF were calculated: its equivalent serial capacitance $C = \frac{1}{2\pi f_0 RQ}$ and inductance $L = \frac{RQ}{2\pi f_0}$.

The operation of the EC-QCL laser, function generator and lock-in amplifier was controlled using a PC notebook computer and serial RS232 interfaces. Digitization of the analog signals was performed using the National Instruments DAQCard 6062E, and LabView programs were used to run the measurements. The QEPAS spectrophone was enclosed in a compact, vacuum-tight gas cell equipped with two ZnSe windows with 4–12 μm AR coating. The pressure inside this cell was controlled and the gas flow was measured using an MKS Type 649A device. All the measurements were performed at a 750 Torr pressure. We used two spectrophones in this work, both designed as shown in Fig. 1 but having different dimensions of the microresonator tubes, which are reported in Table 1 along with the QTF dimensions and measured electrical parameters.

3 Laser characterization and H_2O detection

The laser power measured behind the cell containing the spectrophone at a ×1 laser scan speed is shown in Fig. 3. The total power loss from the optical elements and the pinhole was ∼50%. Our measurements indicate that 2% to 5% of the laser radiation was lost when the laser beam passed the spectrophone, in the absence of any cell window losses. This radiation was eventually absorbed by the spectrophone and the gas cell elements and created an acoustic background at the modulation frequency, related to the laser power but not due to the gas absorption. Therefore, the detection sensitivity in the reported experiments was determined by this background and especially its stability rather than by the QTF thermal noise.

An accurate calibration of the spectral scan was performed using the QEPAS signal from atmospheric water vapor (45% relative humidity at +21°C, 1.1% H_2O by volume). The HITRAN database was used to identify the observed H_2O lines. The results shown in Fig. 4 for the ×1 scan speed confirm the spectral range specified by the manufacturer and near-linear wavenumber tuning with time. The faster scans have the same tuning curve if the time scale is stretched according to the scan rate multiple.

In order to collect the data depicted in Fig. 4a, the lock-in amplifier time constant was set to 3 ms and the filter slope to 12 dB/oct, corresponding to an equivalent noise bandwidth of $\Delta f = 83.3$ Hz. It was verified that with such integration parameters the observed spectral lines were not distorted by the lock-in detection. Their width at ×1 scan rate was determined by the laser linewidth, which was found to be ∼1.5 cm^{-1} in the 1.6% to 7% duty cycle range (0.5 to 2.14 μs pulses). At the ×6 scan rate, the spectral lines have exponentially decaying tails. Such a tail of the 1244.1 cm^{-1} absorption line is shown in Fig. 4(c). The measured decay time 39 ± 2 ms is in a good agreement with $\tau = 41.7$ ms from (3) and the data in Table 1.

When the lock-in bandwidth is wider than the resonant curve of the QTF based spectrophone, the noise cannot be

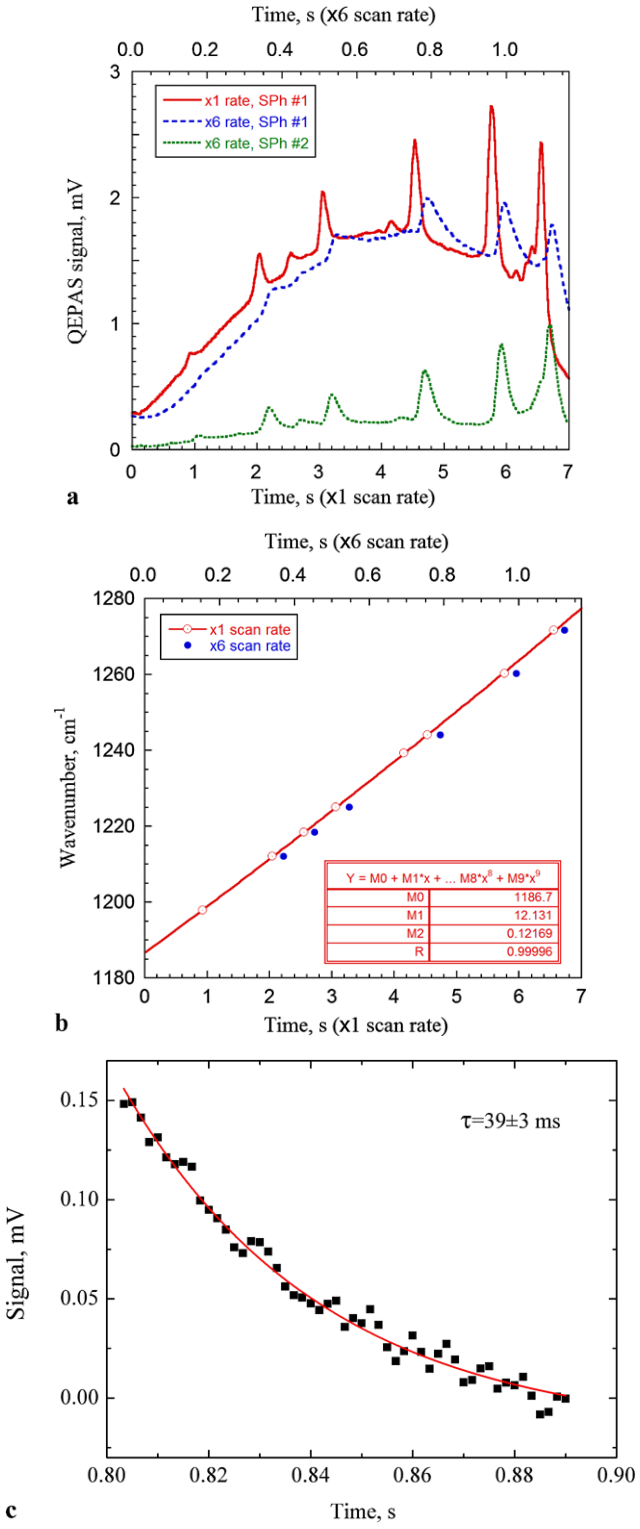

Fig. 4 (**a**) QEPAS signal (voltage rms from the transimpedance amplifier) acquired during the laser wavelength scan over the full tuning range. Time "0" marks the turning point between two directions of the scan. The specified 1196–1281 cm^{-1} spectral range is covered between 0.75 s and 7.25 s. Each trace is the result of averaging data from 10 scans. "SPh" identifies the spectrophone. (**b**) The spectral scan calibration based on the data from (**a**). (**c**) The 1244.1 cm^{-1} absorption line tail (×6, SPh#1) and its exponential fit after background subtraction

calculated using (4) from [2]. Instead, the noise power density should be integrated over the QTF resonant curve. Such an integration results in

$$\sqrt{\langle V_N^2 \rangle} = R_g \sqrt{\frac{k_B T}{L}} \tag{2a}$$

Thus, the QTF thermal noise in this detection mode does not depend on the dissipative losses, but only on the equivalent mass of the oscillator. However, L is not a directly measured parameter. It is more convenient to express noise in terms of the measured parameters:

$$\sqrt{\langle V_N^2 \rangle} = R_g \sqrt{\frac{2\pi k_B T f_0}{RQ}} \tag{2b}$$

The total fundamental noise also includes the gain resistor noise and the operational amplifier noise, integrated over the full lock-in detector bandwidth. However, the power density of these noise sources is usually low and therefore expanding the detection bandwidth beyond the QTF response does not significantly increase the noise level. Indeed, the experimentally measured noise level (RMS of short term point-to-point scatter) was in the 9–11 μV range, in agreement with the theoretically estimated thermal noise of 9 μV.

As mentioned before, in the presence of a high background the practical sensitivity of the device is determined rather by the stability of the radiation-related background than by the ripple on its envelope caused by the QTF thermal noise. However, we shall now estimate the normalized noise equivalent absorption coefficient (NNEA) for the H_2O line at 1244.14 cm^{-1} in order to compare the spectrophone performance with previous QEPAS results. Using the spectral simulation tools from the Institute of Atmospheric Optics (Tomsk, Russia) website [5], we concluded that the simulated atmospheric absorption spectra most closely resemble the observed QEPAS spectra when the instrument function is Gaussian with a 1.5 cm^{-1} FWHM. In this case and for our conditions, the optical absorption at 1244.14 cm^{-1} is 8.21×10^{-5} cm^{-1}. The equivalent noise bandwidth (ENBW) of the QTF should be used because it is narrower than the ENBW of the lock-in amplifier in our experiments, and the QTF determines the time response of the sensor. It can be found that the QTF ENBW $= \frac{\pi}{2}\frac{f_0}{Q}$. Assuming 10 μV noise and 3.12 mW power from Fig. 3, we can calculate:

SPh#1: 9.6×10^{-10} cm^{-1} $W/Hz^{1/2}$
SPh#2: 6.3×10^{-10} cm^{-1} $W/Hz^{1/2}$

Hence, the Sph#2 design provides advantages of both sensitivity and time response. To properly compare this ENBW with the wavelength modulation data from earlier publications, the first terms A_1 in a Fourier series for the corresponding periodic functions should be taken into account.

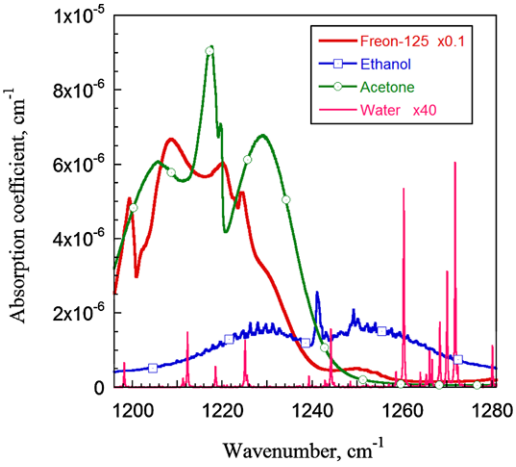

Fig. 5 Absorption spectra of the studied molecules in the tuning range of the EC-QCL. The plots are based on the PNNL database of atmospheric pressure FTIR spectra. All the data are for 1 ppmv concentration, and the absorption coefficient is converted to base e units

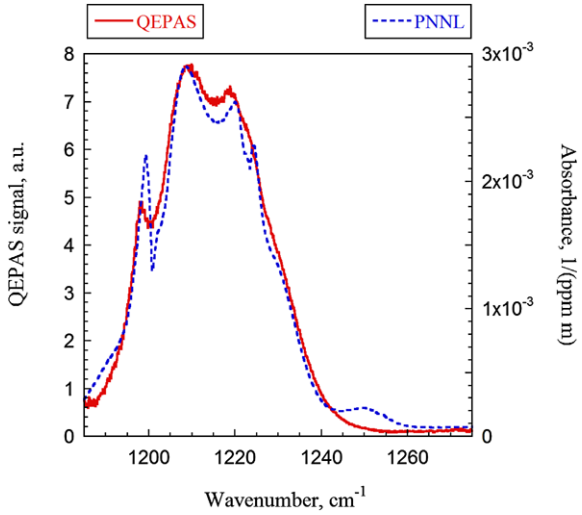

Fig. 6 QEPAS spectrum of freon-125 acquired at the ×6 scan rate compared to the FTIR spectrum obtained from the PNNL database

It can be calculated that for a rectangular wave of average power P and a duty cycle k $A_1 = 2P\frac{\sin(k\pi)}{k\pi}$. For our experimental conditions with $k = 0.07$, $A_1 \approx 2P$. For a sine wave $A_1 = P$, and the $2f$ wavelength modulation signal for a Lorentzian absorption line at the optimum modulation amplitude is $\approx 0.7P$ according to our numerical calculations. Thus, the correction factor from AM—short pulses to a WM—sine wave QEPAS sensitivity is 2.86. If this factor is taken into account, the observed NNEA for SPh#1 corresponds to 2.75×10^{-9} cm^{-1} W/Hz$^{1/2}$. The sensitivity reported in [6] was 3.8×10^{-9} cm^{-1} W/Hz$^{1/2}$, if reduced to a single optical path. Hence, the present sensitivity is in agreement with earlier results but improved because of the adjusted spectrophone dimensions.

4 Detection of larger molecules: pentafluoroethane, acetone, ethanol

The real advantages of an EC-QCL are revealed when detecting large molecules with spectrally unresolved absorption bands. Spectral identification of such molecules requires detection of the bands' envelopes covering 50–200 cm^{-1}. Figure 5 shows absorption bands of pentafluoroethane (freon-125), acetone, and ethanol from the PNNL spectral library [7] in the tuning range of the laser.

For the sensor characterization, we used gas cylinders with 15 ppmv freon-125 in N_2 and 200 ppmv acetone in N_2. As a source of ethanol vapor, a syringe filled with ethanol and having a ~1 mm diameter opening was used. The ethanol concentration in a flow of gas was calculated based on the known diffusion coefficient and the gas flow rate. The measurements were performed using SPh#1, although Sp #2 would likely deliver a better performance. Disregarding some smearing due to the limited spectral (laser) and temporal (spectrophone) resolution, the acquired spectra show close resemblance to the reference FTIR spectra even at the highest 78.5 cm^{-1}/s scan rate. As an example, Fig. 6 shows freon-125 data after background subtraction and correction for the varying optical power.

The spectral data analysis was based on the general linear fit (GLF) method and the corresponding "Virtual Instrument" (VI) from the National Instruments LabView package. The experimentally acquired spectral data were represented as a linear combination of absorption (or QEPAS) spectra of individual molecular compounds, plus a frequency-dependent background signal:

$$S(\nu) = \sum_{i=0}^{n} a_i S_i(\nu) \tag{3}$$

Here $S(\nu)$ is the measured QEPAS signal as a function of the optical frequency, $S_0(\nu)$ is the spectral dependence of the laser-related background (identical to the laser power curve depicted in Fig. 3), and $S_i(\nu)$ for $i = 1$ to n represent the absorption of n molecular species. In our case, there were 4 such functions corresponding to freon-125, acetone, ethanol, and H_2O. In practice, ν was not measured directly but determined by the time delay t from the laser scan start and hence, $S(t)$ and $S_i(t)$ were actually used. In order to acquire $S_i(t)$, the QEPAS data from 10 to 15 laser scans of the corresponding gas mixture were averaged, and then a similarly averaged pure nitrogen data (background) subtracted. Thus, $S_i(t)$ already included the information about the laser power during a scan. The coefficient a_i is proportional to the concentration of the i-th compound, if we assume that there is no cross-correlation, which, in principle, may occur because of the mutual influence of molecular species in the

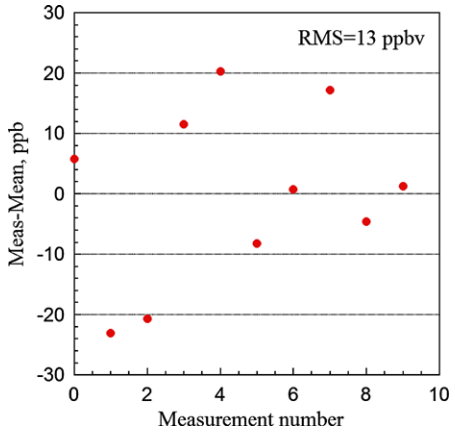

Fig. 7 Scatter of the freon-125 concentration derived from consecutive measurements (single laser scans) using the general linear fit (GLF) technique. The highest (×6) scan rate of 77.3 cm^{-1}/s was used

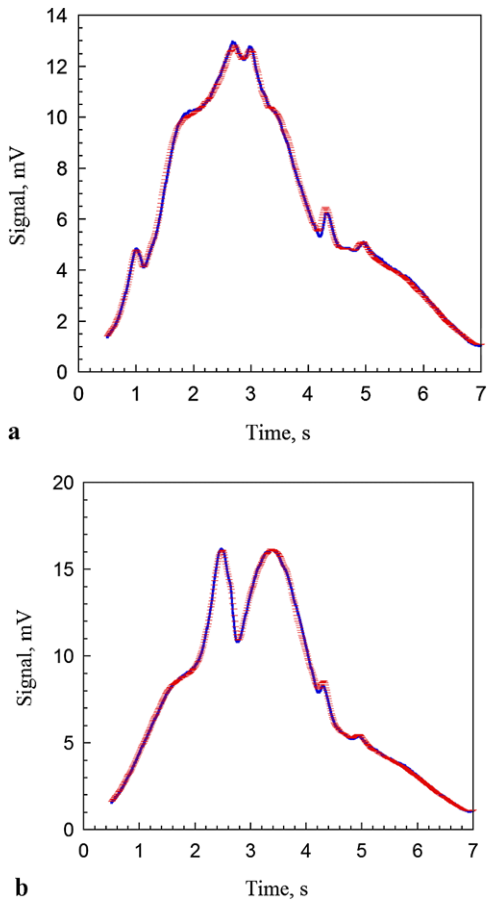

Fig. 8 Experimental points (horizontal dashes) and GLF (*solid curve*) for (**a**) freon-125 and ethanol in a N_2 carrier gas, and (**b**) acetone and ethanol in a N_2 carrier gas. Data were acquired at ×1 scan rate

gas on the V–T relaxation rate. For simpler data processing, only the in-phase component of the signal was used. This resulted in no more than a 30% decrease of the signal.

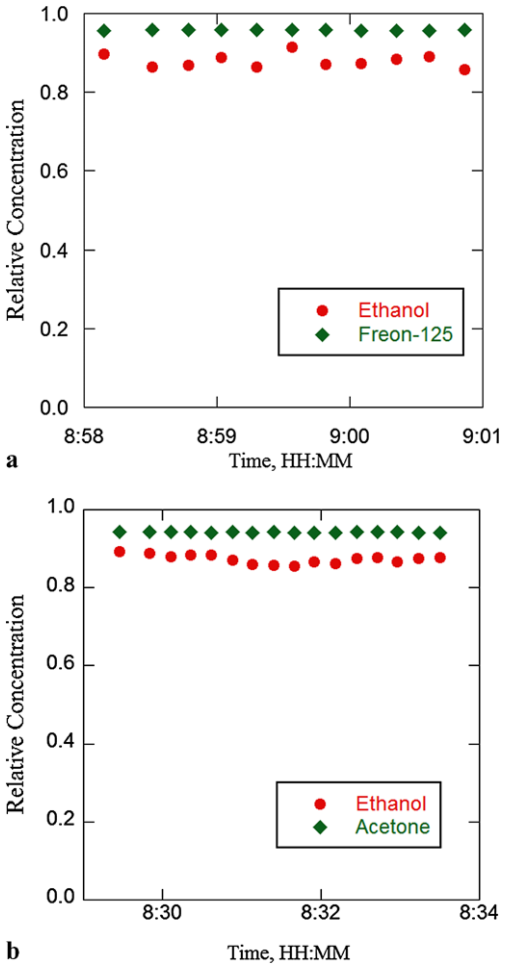

Fig. 9 Relative concentrations (a_i coefficients in (3)) derived from consecutive measurements using the GLF technique applied to mixtures each containing two absorbing components: (**a**) freon-125 and ethanol, and (**b**) acetone and ethanol

In order to evaluate the sensor precision, repeated measurements of the same gas mixture were performed. The scatter of results for a 15 ppmv freon-125 in N_2 mixture is shown in Fig. 7, yielding a precision of $\sigma = 13$ ppbv. Similar measurements for 200 ppmv acetone in N_2 yield $\sigma = 250$ ppbv. Thus, in both cases the achieved relative precision is ∼0.1% of the concentration, most likely reflecting the stability of the laser source. This is a remarkably good number for a pulsed laser system considering that the measurements did not involve normalization to the instant laser power.

The described data processing technique was then applied to gas mixtures containing two optically absorbing chemical species. A simple ethanol vapor generator (syringe containing ethanol and having a ∼1 mm diameter opening) was inserted into the stream of one of the calibrated gas mixtures mentioned above. The acquired QEPAS data fitted with a linear combination of the corresponding $S_i(t)$ functions are shown in Fig. 8. The scatter of the measured concentrations is depicted in Fig. 9. As expected, concentrations from

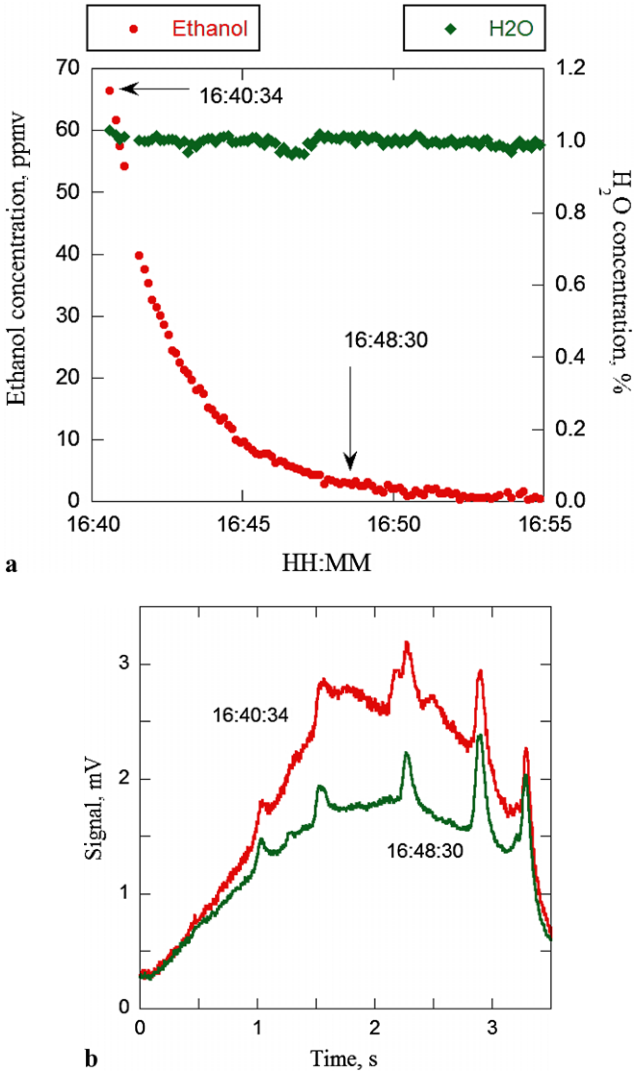

Fig. 10 (**a**) Evolution of the ethanol and water vapor concentrations in the system when it is flushed by a 70 sccm air flow; (**b**) single scans acquired at two different times, as indicated by *arrows* in (**a**)

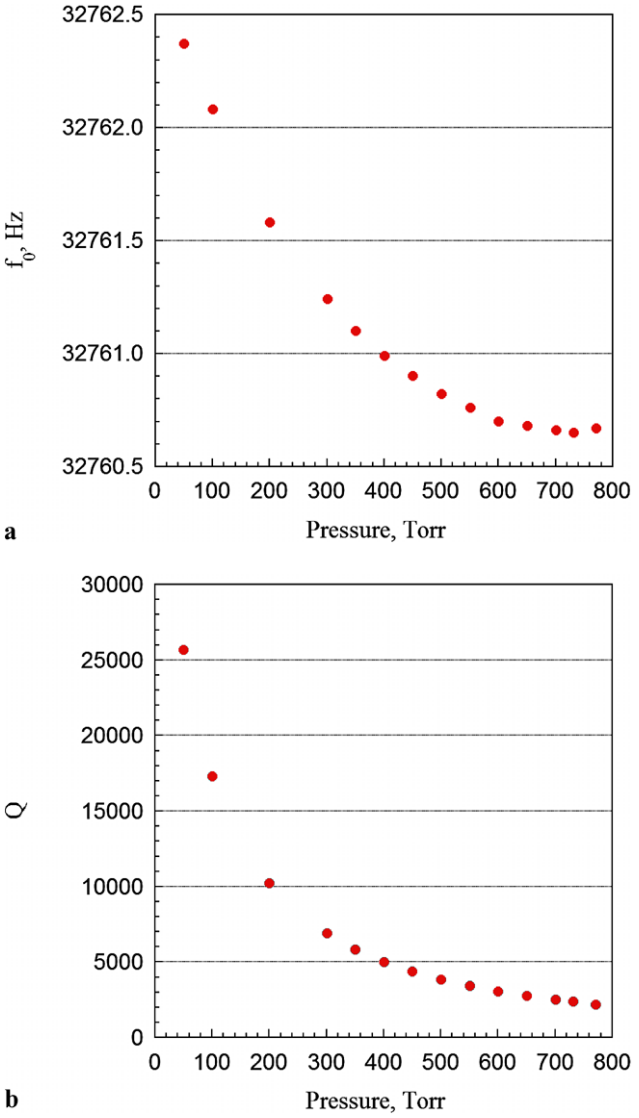

Fig. 11 Properties of SPh#2 as a function of dry nitrogen pressure: (**a**) resonant frequency, (**b**) quality factor

gas standards are more stable than the ethanol vapor concentration from a primitive home-made source. The scatter of the freon-125 concentration in the mixture shown in Fig. 9(a) yields a precision of $\sigma = 15$ ppbv, which is practically the same as for freon-125 in pure nitrogen.

An additional experiment was performed to see how well the evolution of concentration can be monitored using this sensor. The gas system was briefly exposed to a high concentration of ethanol and then flushed with a 70 sccm flow of ambient air (+20°C, 43% relative humidity). While the ethanol was gradually removed from the gas system, QEPAS data were repeatedly acquired at the $\times 2$ laser scanning rate. The results are shown in Fig. 10, as well as two examples of the spectral data. Although the ethanol spectral features cannot be observed visually in the 16:48:30 spectrum, which is dominated by background and water lines, the ethanol concentration is reliably retrieved from such data using GLF, and it is still much higher than the noise floor. The plot in Fig. 10(a) also shows a close-to-constant retrieved H_2O concentration. The precision of the H_2O measurements is lower because its absorption features cover only a small fraction of the total spectral scan, hence involving fewer informative data points.

5 Spectrophone properties as a function of the gas pressure

The Q-factor of an organ pipe type acoustic resonator is proportional to the square root of the gas density [8]. Acoustic coupling between the gas in the tubes and the QTF will

also be stronger at higher gas density because of the larger momentum carried by the gas flow. Therefore, we can expect that the spectrophone properties will change when the gas pressure varies. We performed the SPh#2 parameter measurements at different N_2 pressures, and the results are shown in Fig. 11.

The dependence of the resonant frequency on the gas pressure is very different from a bare QTF [2] or a QTF with frequency-detuned microresonator where it is practically linear. A qualitative explanation is frequency pulling of the QTF resonance to the resonance of the acoustic resonator at higher pressures where both acoustic coupling and the Q-factor of the tubes are higher. The resonant frequency of the tubes does not depend on the gas pressure, and therefore the spectrophone resonance stays almost constant in the 650–800 Torr range. The changes in f_0 are negligible compared to the resonance width at these pressures where the $Q < 3000$. Indeed, the FWHM of the amplitude response of the oscillator is $\Delta f = \sqrt{3}\frac{f_0}{Q}$, and for a $Q = 3000$ it is $\sim$19 Hz. Hence, neither precise pressure control nor frequent adjustments of the modulation frequency is needed.

6 Conclusions

We demonstrated that a QEPAS detector can be used to acquire spectral data at a much faster rate than it was considered possible in earlier publications, with a time constant as short as $\sim$15 ms. A strong decrease of the Q-factor of the spectrophone caused by efficient acoustic coupling between the QTF and an acoustic resonator does not reduce the QEPAS detection sensitivity. To the contrary, the fundamental SNR normalized to the detection bandwidth increases. On the other hand, the spectrophone parameters (its resonant frequency and Q-factor) become more sensitive to the gas composition and temperature. Besides, sensitivity to environmental acoustic background is expected to become higher, although it was not directly observed in this work. Therefore, the design of a QEPAS spectrophone must be performed considering all the requirements and conditions of a specific application.

Acknowledgements The authors acknowledge Dmitry Serebriakov (Institute of Spectroscopy, Russia) for helpful discussions and David Thomazy (Rice University) for the technical support. The Rice University group acknowledges a sub-contract from Daylight Solutions, Inc and SRI International, the financial support from a National Science Foundation ERC MIRTHE award, and grant C-0586 from The Welch Foundation. This paper is based upon work supported by the Defense Advanced Research Projects Agency's Strategic Technology Office (STO) under contract HR0011-09-C-0049 "Chemical Identification for Surveillance and Tracking ('ChemIST')". The views and conclusions contained in this document are those of the authors and should not be interpreted as representing the official policies, either expressed or implied, of the Defense Advanced Research Projects Agency or the U.S. Government.

References

1. A.A. Kosterev, Yu.A. Bakhirkin, R.F. Curl, F.K. Tittel, Opt. Lett. **27**, 1902 (2002)
2. A. A Kosterev, F.K. Tittel, D.V. Serebryakov, A.L. Malinovsky, I.V. Morozov, Rev. Sci. Instrum. **76**, 043105 (2005)
3. D.V. Serebryakov, I.V. Morozov, A.A. Kosterev, V.S. Letokhov, Laser micro-photoacoustic detector of trace ammonia in atmosphere. Kvant. Elektron. **40**, 167–172 (2010) (in Russian)
4. N. Petra, J. Zweck, A.A. Kosterev, S.E. Minkoff, D. Thomazy, Appl. Phys. B **94**, 673 (2009)
5. SPECTRA Information System, http://spectra.iao.ru
6. A. A Kosterev, F.K. Tittel, T.S. Knittel, A. Cowie, J.D. Tate, in *Laser Applications to Chemical, Security and Environmental Analysis 2006 Technical Digest* (The Optical Society of America, Washington, 2006)
7. S.W. Sharpe, T.J. Johnson, R.L. Sams, P.M. Chu, G.C. Rhoderick, P.A. Johnson, Appl. Spectrosc. **58**, 1452 (2004). See also https://secure2.pnl.gov/nsd/nsd.nsf/Welcome
8. A.B. Pippard, in *The Physics of Vibration*, vol. 1 (Cambridge University Press, Cambridge, 1978), Chap. 7